Hindawi
Journal of Advanced Transportation
Volume 2022, Article ID 8233424, 14 pages
https://doi.org/10.1155/2022/8233424

*Research Article*

# Conflict Probability Prediction and Safety Assessment of Straight-Left Traffic Flow at Signalized Intersections

**Yingying Ma, Zihao Zhang, and Jiabin Wu**

*Department of Transportation Engineering, South China University of Technology, Guangzhou 510641, China*

Correspondence should be addressed to Jiabin Wu; 13670000003@sina.cn

Received 30 September 2021; Revised 24 March 2022; Accepted 28 April 2022; Published 25 June 2022

Academic Editor: Geqi Qi



The safety of signalized intersections is of great concern. To allow for an effective evaluation measure on the safety level of intersections, traffic conflict analysis methods are commonly used. However, the existing literature has mainly focused on the statistical prediction of conflicts by using surrogate measurements, among which the spatial-temporal characteristics of the potential conflicts have been less addressed. In addition, most of the relevant studies rely on precise trajectory data, and the results could be limited to engineering applications when real-time/comprehensive trajectory data are not available. To address these issues, this study proposes a SICP (signalized intersection conflict probability) model to predict a straight-left traffic flow conflict with a spatial-temporal distribution in the heat map, which could effectively evaluate the traffic safety of the existing or prebuilt signalized intersections on urban roads. Firstly, the impact of vehicle movement characteristics on traffic conflict at signalized intersections was considered by incorporating the vehicle movement trajectory. Secondly, the signal phase was categorized in several stages (each phase contains switching and nonswitching stages); then, a vehicle-vehicle conflicts probability prediction model was established by integrating both horizontal and vertical arrival probability. Finally, to validate the performance of the proposed model, the measured data were collected from the intersection of Wushan road and Yuehan road in Tianhe District, Guangzhou, China. SSAM ( Surrogate Safety Assessment Model ) traffic conflict simulation was used to analyze the traffic conflict in the actual data and compared to the SICP model. A case study was conducted to reveal the evolution mechanism of the conflict risk coefficient at the signalized intersection and to estimate the safety status under the various security optimization strategies. The experimental results verified the effectiveness of the SICP model, indicating that the proposed model is effective in evaluating the safety level of existing or prebuilt signalized intersections.

## 1. Introduction

As the bottleneck of the urban road network, signalized intersections play an important role in the operation of urban transportation, as various road users exist, such as motor vehicles, nonmotor vehicles, pedestrians, and other road users. However, signalized intersections are nodes with frequent traffic conflicts and congestion, as well as the common place of traffic accidents. As a key component to realize the distribution of the right way at intersections, signal control facilities are responsible for maintaining the normal operation of the traffic order. Although the existing urban traffic managers separate the right-going and left-turning traffic flows at signalized intersections in time or space, there are still some small-sized intersections with right-left mixed lanes, or the straight-going and left-turning traffic flows are released at the same time due to unreasonable signal timing. At this time, there is the right-of-way competition between the straight-going traffic flow and the left-turning traffic flow, and this is an important cause of the frequent blocking and traffic conflicts at intersections, as shown in Figure 1(a). In addition, all-red intervals of some signalized intersections are not set or are too short to clear the vehicles of the last phase, which leads to serious conflicts during the phase switch, as shown in Figure 1(b). Therefore, the frequency and severity of traffic conflicts at such signalized intersections are higher than those in other areas. Therefore, traffic conflicts and collisions are more likely to

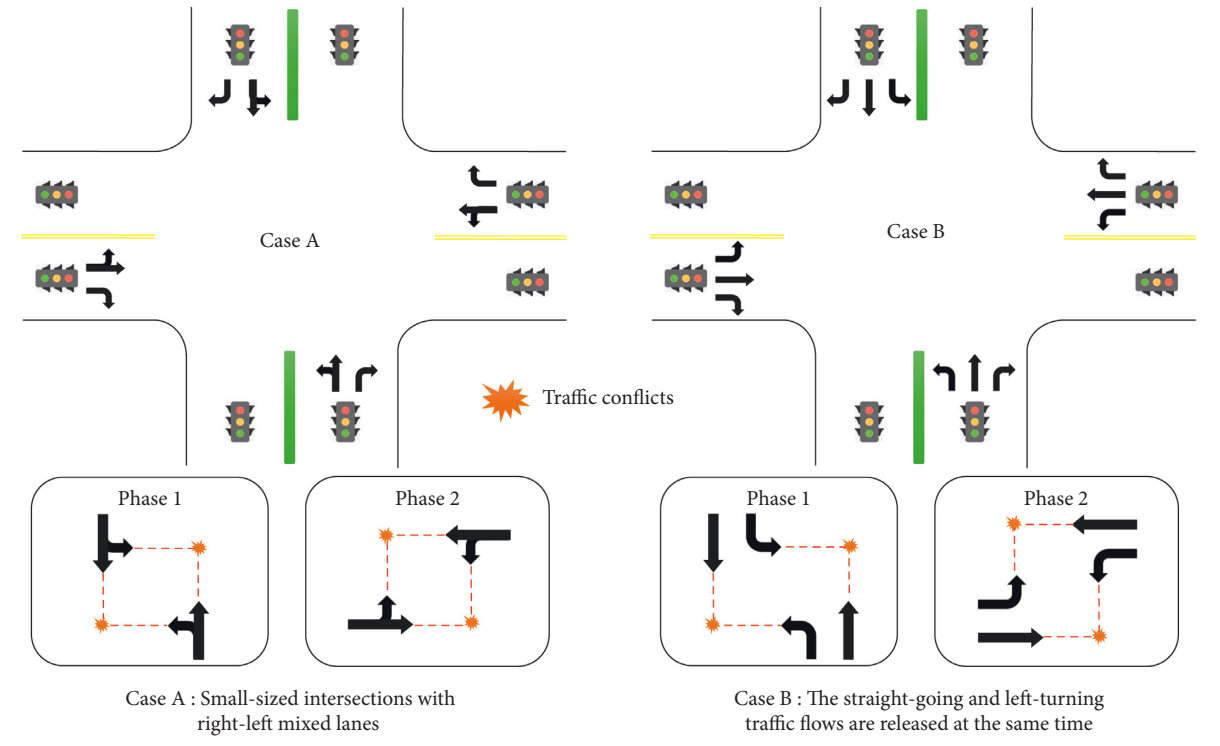


(a)

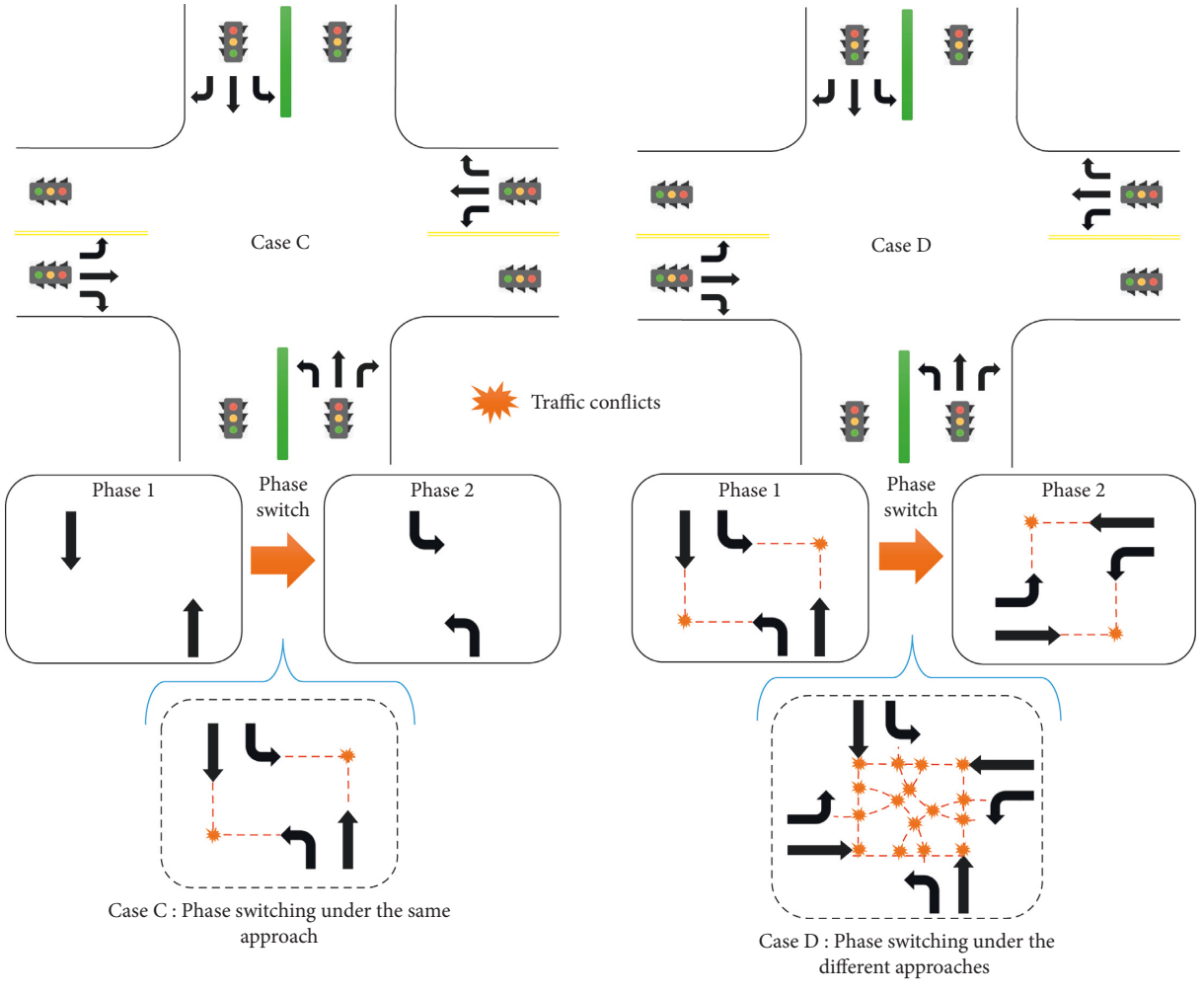


(b)

Figure 1: The traffic conflicts of some signalized intersections in one signal cycle. (a) Two common cases of traffic conflicts at signalized intersections during a phase. (b) Two common cases of traffic conflicts at signalized intersections during the phase switch.

occur at signalized intersections with the simultaneous release of straight and left traffic flow, and the safety assessment of this issue deserves more attention.

The safety evaluation methods of signalized intersections are mainly divided into two categories: one is the direct evaluation method based on traffic accident statistics, and the other is the indirect evaluation method based on traffic conflict analysis. The direct evaluation methods mainly include empirical modelling [1], gray evaluation [2], regression modelling [3], and other methods. The expected number of traffic accidents is taken as the evaluation index, which strongly relies on the historical accident data. By analyzing the historical data of road traffic accidents in 20 European countries, Al-Ghamdi [4] studied the correlation between the death toll of road traffic accidents and the population and the number of motor vehicles, performed regression analysis, and proposed the Smeed model. Guo et al. [5] collected historical traffic accident data by mobile apps, established an improved k-means algorithm, evaluated road traffic safety, and identified traffic accident black spots. Chen et al. [6] collected traffic and accident data from 246 nonsignalized intersections and proposed a generalized negative binomial regression model based on zero censorings to comprehensively evaluate the safety of intersections. Although the application of this method is direct and simple, the drawback is also acknowledged that it requires a significant amount of high-quality accident statistical data in most cases. Therefore, the application of the direct evaluation method in traffic safety analysis is somewhat limited due to the difficulties of obtaining traffic accident data, its unstable quality, and long collection period.

In contrast, indirect evaluation methods based on traffic conflict analysis are more widely used in traffic safety analysis. These studies use the frequency and severity of traffic conflicts to indirectly reflect the level of traffic safety, which mainly focuses on the effectiveness of traffic conflicts [7–19], traffic conflict evaluation indicators [20, 21], and data methods [22, 23]. To facilitate the extension and application of the definition of traffic conflict in practice, scholars have proposed a variety of traffic conflict indicators to quantify the proximity and interaction between two or more road users in time or space. The most commonly used conflict indicators include the time to collision (TTC) [24, 25], the postencroachment time (PET) [26–28], and the stopping distance index (SDI) [29–31]. For example, Hayward [25] proposed TTC as a measurement index of traffic conflict, which is defined as the time to collision when two vehicles maintain their existing speed and direction unchanged, to evaluate the traffic safety level of intersections. Mohamed et al. [32] collected TTC and the traffic parameters of each signal cycle at signal intersections and proposed a safety performance function based on traffic conflict by using a generalized linear model, which evaluated the traffic safety status of signalized intersections. Guo [33] collected traffic conflict data of vehicles at signalized intersections and proposed safety evaluation methods of conflicts between motor vehicles and motor vehicles, motor vehicles and nonmotor vehicles, and motor vehicles and pedestrians at signalized intersections based on the Bayesian method. Ma et al. [34] built a traffic conflict identification model based on the PET algorithm in ramp merging areas, considering vehicle movement information and the influence of vehicle size on traffic conflict and provided a method for determining the severity of traffic conflict. Laureshyn et al. [35] proposed a traffic conflict measurement method based on extended Delta-V to evaluate the safety status of various intersections, from the perspective of traffic accident severity. Oh et al. [30] proposed stopping sight distances based on SDI to estimate whether a given car-following condition is safe. Hyden [36] proposed time to accident (TA) as an indicator to identify road traffic conflicts and then evaluated road safety. This kind of method is widely used, of which the model is stable and flexible, and the evaluation index is diversified, but it does not consider the actual size of the vehicle and is unable to evaluate the future situation of intersections. In addition, most of the previous studies deeply rely on real-time vehicle trajectory data, which are hard to access in engineering applications. Thus, these methods can only evaluate the safety of the existing signalized intersections and fail to assess the safety level of the design scheme or optimization scheme of the signalized intersections. Furthermore, few studies have focused on the spatial-temporal characteristics of the potential conflicts at signalized intersections, and instead they tend to pay more attention to the recognition accuracy of traffic conflicts. Finally, according to our latest knowledge, there is no literature concerning traffic conflict when two phases switch, which may be the most serious period of traffic conflict.

To address the above issues, this paper proposes a new method of conflict probability prediction for signalized intersections, considering the micro operation characteristics of vehicles based on their actual size. The best feature of the proposed model is that it has low traffic data requirements and only needs traffic flow and signal timing parameters instead of real-time vehicle trajectories or an enormous body of historical data. In other words, the model can not only evaluate the existing signalized intersections, but also analyze the traffic conflicts of prebuilt signalized intersections as long as the design scheme provides the related data. The secondary superiority is to consider the spatial-temporal characteristics of the potential conflicts to evaluate the comprehensive safety level of signalized intersections. On the one hand, the spatial distribution of traffic conflicts is deduced by merging areas of different vehicle running trajectories. Besides, the signal timing is divided into several stages based on the changes in the spatial distribution of the traffic conflicts. Another crucial creativity of this study is that the proposed model is especially concerned with traffic conflicts during phase switching, which is a very important period but is usually ignored in other researches. The simulation experiment and case analysis results are conducted to verify the effectiveness of the SICP model. These findings can provide theoretical and technical support for the channelization design and signal timing optimization of signalized intersections for traffic engineers.

The remainder of this paper is arranged as follows. Section 2 describes how to construct the cell system of a signalized intersection. Section 3 explains the modelling

process of the SICP model and the calculation of the safety assessment index. Section 4 gives some comparative experiments and results based on the actual data. Three typical case studies and discussions are illustrated in Section 5. Eventually, this paper ends with some conclusions and future work in Section 6.

## 2. Analysis on Micro Operation Characteristics of Vehicles at Signalized Intersections

*2.1. Cell Division and Its Approximation.* To effectively evaluate the internal traffic safety status of a signalized intersection, a two-dimensional Cartesian plane coordinate system is constructed by taking the intersection of the east-west direction and the north-south direction of the intersection as the coordinate origin. The east approach road is the positive direction of the $X$-axis, while the north approach road is the positive direction of the $Y$-axis. It is assumed that the width of the approach and exit lanes in all directions of the intersection are symmetrical. Let $M$ and $N$ denote the length and width of the intersection, respectively. $M-1$ and $N-1$ points are evenly inserted on the $X$-axis and $Y$-axis, respectively, and the intersection conflict area is evenly divided into $M \times N$ cells, as shown in Figure 2.

$$\begin{aligned} -\frac{M}{2} &= x_0 < \cdots < x_j < \cdots < x_n = \frac{M}{2}, \\ -\frac{N}{2} &= y_0 < \cdots < y_i < \cdots < y_m = \frac{N}{2}, \end{aligned} \tag{1}$$

where $i = 1, 2, \ldots, m$, $j = 1, 2, \ldots, n$. $m$ and $n$ are positive integers, and its value must meet that the length and width of each cell are less than the vehicle width to reflect the arrival of vehicles. At this time, vehicles occupying any part of a cell are regarded as vehicles arriving at the cell.

In the coordinate system, the cell in row $i$ and column $j$ is denoted as Rec$(i, j)$. The probability of the vehicle occupying the cell can be approximately regarded as the probability of the vehicle appearing in the centroid of the cell. $(x_{ij}, y_{ij})$ is used to represent the centroid coordinates of the cell Rec$(i, j)$, as shown in

$$x_{ij} = \frac{x_i + x_{i+1}}{2}, y_{ij} = \frac{y_j + y_{j+1}}{2}. \tag{2}$$

*2.2. Analysis of the Vehicle Trajectories.* Taking the signalized intersection with six two-way lanes where straight and left-turn vehicles are released simultaneously as an example, this paper describes the vehicle trajectories under different signal phases by corresponding mathematical expressions, as shown in Figure 3. Additionally, the trajectory equation used in this paper can also be applied to straight and left turn mixed traffic and the signalized intersections of other geometric conditions.

According to the lane function setting of the intersection, the vehicle trajectory equation of each approach is established. Taking the signalized intersection in Figure 3 as an example, let a $(a = 3)$ denote the number of lanes at each approach road. The lanes are numbered from inside to outside in the order of small to large; that is, the lane number $h = 1, \ldots, a$. Then, the vehicle trajectory equations of going straight and turning left and right at each approach road are as follows:

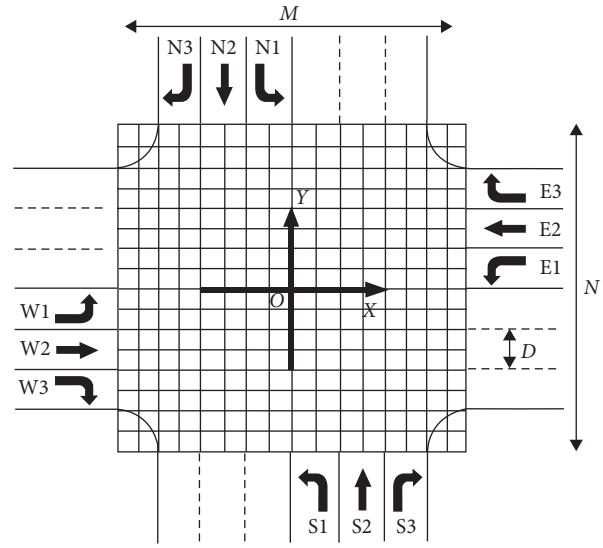


Figure 2: Coordinate system and cell division of conflict area in a signalized intersection.

$$\begin{aligned} \frac{A}{2} + (h-1)D \le y_{ij} \le \frac{A}{2} + hD, \\ \left(x_{ij} - x_{dw}\right)^2 + \left(y_{ij} - y_{dw}\right)^2 = R_w^2, \end{aligned} \tag{3}$$

where $R_w$ denotes the left turning or right turning radius of the vehicle in each approach, and $R_w \in [R_{dw} - 0.5D, R_{dw} + 0.5D]$. $R_{dw}$ denotes the designed radius of left-turning or right-turning of the vehicle in each approach. $(x_{dw}, y_{dw})$ denotes the center coordinates of the turning track circle at each approach. $d$ represents the direction of the approach, and $d = \{d_1, d_2, d_3, d_4\}$ denote the directions east, west, south, and north, respectively. $w = \{l, r\}$ indicate the left and right turn directions, respectively. $D$ denotes the width of the single lane, and $A$ denotes the width of the median.

## 3. Signalized Intersection Conflict Probability Model

*3.1. Signal Phase Decomposition considering the Temporal and Spatial Evolution of Traffic Conflict.* In this paper, the SICP model divides signal phases at intersections based on the evolution of conflict mechanisms. Some small intersections may not set the all-red time or the all-red time is too short. When the signal phase switches periodically, the vehicles in the previous phase often fail to leave the intersection in time, which is likely to cause traffic conflicts with the vehicles starting in the next phase. During this period, the traffic conflict situation is relatively complex, and the composition of participants in the conflict changes. Thus, this process is

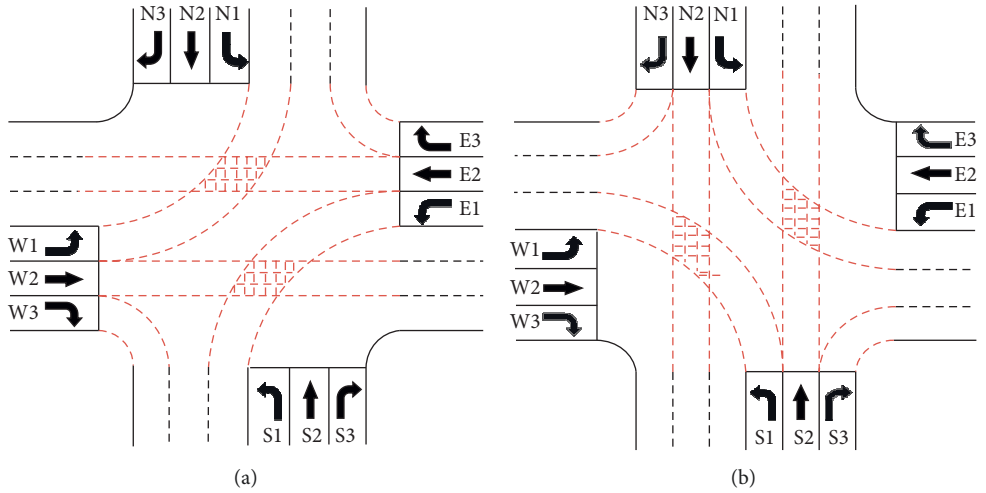


Figure 3: Vehicle trajectories at a signalized intersection. (a) Phase 1: vehicle trajectories of east-west approach. (b) Phase 2: vehicle trajectories of north-south approach.

defined as a phase switching stage, and other processes of the same phase are called the nonphase switching stage. Their critical time is the moment when the vehicles at the end of the previous phase leave the intersection.

To describe the generality of the phase division, the phase number in the signal timing scheme is set as $Z$. Each signal cycle can be divided into $2Z$ phase stages based on the evolution of the conflict probability. That is, one phase includes the phase switching stage and nonphase switching stage, as shown in Figure 4. Suppose $T_i$ denotes the duration of the $i$th phase, $L_j$ denotes the distance of each traffic flow in the previous phase from the stop line to leave the intersection, and $v_j$ denotes the average driving speed of each traffic flow in the previous phase. The durations of the phase switching stage and nonphase switching stage in the $i$th phase are

$$T_{i1} = \max\left\{\frac{L_1}{v_1}, \ldots, \frac{L_j}{v_j}\right\},$$
$$T_{i2} = T_i - T_{i1}, \tag{4}$$

where $T_{i1}$ and $T_{i2}$ are the duration of the phase switching phase and the nonphase switching phase in phase number $i$, respectively. For example, $T_{11}$ and $T_{21}$ denote the duration of the phase switching stage, and $T_{12}$ and $T_{22}$ denote the duration of the nonphase switching stage. $j$ is the number of traffic flow at a signalized intersection, $i = 1, \ldots, Z$.

*3.2. Conflict Probability Models considering Micro Operation Characteristics of Vehicles.* Considering the rear-end collision and the front or side collision from different angles, a conflict probability model of the vehicle for any cell at signalized intersections is established. Let $k$ denote the vehicle trajectory, and there are at most three vehicle trajectories passing through a cell simultaneously ($k \le 3$) [28]. Then, the probability of traffic conflict in cell Rec($i$, $j$) is

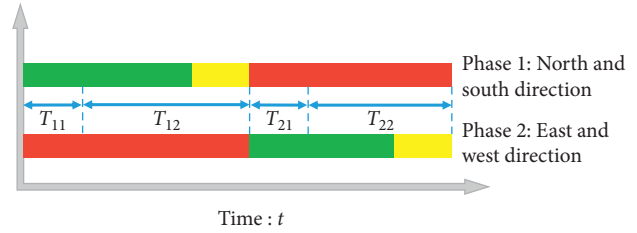


Figure 4: Diagram of phase decomposition of the signalized intersection (green, yellow, and red indicate the duration of the green, yellow, and red lights respectively).

$$P_{ij} = \sum_{k=1}^{3} \left(P_{\mathrm{Aij}}^{k}\right)^2 + P_{\mathrm{Aij}}^{1} \times P_{\mathrm{Aij}}^{2} + P_{\mathrm{Aij}}^{1} \times P_{\mathrm{Aij}}^{3} + P_{\mathrm{Aij}}^{2} \times P_{\mathrm{Aij}}^{3} + P_{\mathrm{Aij}}^{1} \times P_{\mathrm{Aij}}^{2} \times P_{\mathrm{Aij}}^{3},$$
$$P_{\mathrm{Aij}}^{k} = P_{\mathrm{Dij}}^{k} \times P_{\mathrm{Lij}}^{k}, k \le 3, \tag{5}$$

where $P_{ij}$ denotes the conflict probability of cell Rec($i$, $j$), and $P_{A_{ij}}^{k}$ denotes the probability that the vehicle reaches cell Rec($i$, $j$) along with vehicle trajectory $k$. If there is no traffic flow arriving at cell Rec($i$, $j$) along the vehicle trajectory, the arrival probability of the vehicle in cell Rec($i$, $j$) is 0. $P_{L_{ij}}^{k}$ denotes the longitudinal arrival probability of the vehicle in cell Rec($i$, $j$) along vehicle trajectory $K$; $P_{D_{ij}}^{k}$ denotes the probability that the vehicle appears in cell Rec($i$, $j$) along with vehicle trajectory $k$ due to lateral offset.

*3.2.1. The Longitudinal Arrival Probability of Vehicle considering the Interference of the Signal Light.* It is assumed that most of the vehicles travel along the path set by the motion trajectory equation and ignore the heterogeneity of individual vehicles. The probability of vehicles appearing in the cell outside the coverage area of the vehicle trajectory equation can be approximately zero. For the cell covered by the vehicle trajectory equation, the longitudinal arrival probability of the vehicle in the cell is discussed in two cases

considering the signal light. (1) If the signal light is green or yellow, the vehicles are allowed to enter the intersection, and the longitudinal arrival probability of that in the cell is not zero. (2) If the signal light is red, the vehicles are not allowed to enter the intersection, and the longitudinal arrival probability of that appearing in the cell is zero. Therefore, this paper mainly focuses on the longitudinal arrival probability of the vehicle in the cell in the first case.

Due to the limitation of signal control facilities, the way that the vehicles pass the intersection is mainly divided into two cases: one is to pass after waiting in line, and the other is to pass freely (without stopping to pass). When the signal light turns green from red, the vehicles begin to pass through the intersection successively from stop status, and their headways obey the lognormal distribution model [37]. If the green time is greater than the queue dissipation time, the headway of the vehicles arriving at the intersection in the remaining green time obeys the Poisson distribution model. In a statistical sense, the arrival probability of traffic flow during the green light can be regarded as the weighted result of the arrival probability of the above two types of traffic flows. The proportion of the two types of traffic flow can be determined by the ratio of dissipation time of the queue length to the effective green time. Hence, the longitudinal arrival probability of the vehicle appearing in cell Rec($i$, $j$) along with trajectory $k$ in conflict time $t$ is

$$P_{\mathrm{Lij}}^{k}=\begin{cases}\left(1-\dfrac{g_d}{g_e}\right)\times\left(1-e^{-q_k t}\right)+\dfrac{g_d}{g_e}\times\dfrac{e^{-\left(\ln t-\mu_1\right)^2/2\sigma^2}}{t\sigma_1\sqrt{2\pi}}, g_e>g_d,\\ \dfrac{1}{t\sigma_1\sqrt{2\pi}}e^{-\left(\ln t-\mu_1\right)^2/2\sigma_1^2}, g_e\le g_d,\end{cases} \tag{6}$$

$$g_d=\frac{q_k C}{S},$$

$$t=\min\left\{\frac{L+B}{V_1},\frac{L+B}{V_2}\right\},$$

where $g_d$ is the dissipation time of the queue length, $g_e$ is the effective green time, $q_k$ is the traffic flow along with the vehicle trajectory $k$, $C$ is the signal period, $S$ is the saturation flow rate, and $t$ is the conflict time. If the time difference between the two cars appearing in the same cell successively is less than $t$, it would be seen as a traffic conflict. $\mu_1$ and $\sigma_1^2$ are the moment estimations of expectation and the variance of time headway, respectively. $L$ is the length of the vehicle, $B$ is the width of the vehicle, and $B=f_1B_1+f_2B_2+f_3B_3$. $f_1$, $f_2$ and $f_3$ are the vehicle proportions of small, medium, and large vehicles, respectively. $B_1$, $B_2$, and $B_3$ are the width of a small vehicle, medium vehicle, and large vehicle, respectively. $V_1$ and $V_2$ are the designed speed of the road where traffic flow may cause traffic conflicts. All vehicles are assumed to be small cars during the example verification.

*3.2.2. The Lateral Deviation Probability in Vehicle Trajectory.* Because the driver can not completely avoid operation error, there is a certain deviation (the distance between the centerline of the vehicle and the centerline of the lane) in lane-keeping, and the deviation is subject to a normal distribution [34, 38, 39]. Thus, the probability of straight and turning vehicles appearing in cell Rec($i$, $j$) due to lateral deviation can be obtained from

$$P_{\mathrm{Dij}}=\begin{cases}\displaystyle\int_{y_{ij}+B/2-3D/2-A/2}^{D-B/2}\frac{1}{\sqrt{2\pi}\sigma_2}e^{-\left(y-\mu_2\right)^2/2\sigma_2^2}\mathrm{dy}, y_{ij}\in Z_1,\\ 1, y_{ij}\in Z_2,\\ \displaystyle\int_{y_{ij}+B/2-3D/2-A/2}^{D-B/2}\frac{1}{\sqrt{2\pi}\sigma_2}e^{-\left(y-\mu_2\right)^2/2\sigma_2^2}\mathrm{dy}, y_{ij}\in Z_3,\end{cases} \tag{7}$$

$$P_{\mathrm{Dij}}=\begin{cases}\displaystyle\int_{\left|R_w-R_{dw}-B/2\right|}^{D-B/2}\frac{1}{\sqrt{2\pi}\sigma_2}e^{-\left(R_w-\mu_2\right)^2/2\sigma_2^2}dR_w, R_w\in K_1,\\ 1, R_w\in K_2,\\ \displaystyle\int_{\left|R_w-R_{dw}+B/2\right|}^{D-B/2}\frac{1}{\sqrt{2\pi}\sigma_2}e^{-\left(R_w-\mu_2\right)^2/2\sigma_2^2}dR_w, R_w\in K_3,\end{cases} \tag{8}$$

where $P_{Dij}$ is the probability that the vehicle appears in cell Rec($i$, $j$) due to lateral offset; $\mu_2$ and $\sigma_2^2$ are the mean and variance of the lateral deviation of straight or turning vehicles, respectively. The data can be obtained by fitting the lateral deviation position with the MATLAB toolbox.

### 3.3. Safety Assessment of Signalized Intersections

*3.3.1. Risk Level Classification.* The conflict probability output by the SICP model refers to the probability that two or more vehicles appear in a cell at the same time during the conflict time. Therefore, it can be converted into the ratio between the frequency of traffic conflicts and the traffic volume in the cell within a period (TC/MPCU). Pei et al. [40] conducted statistics on TC/MPCU values of 295 intersections in 33 cities in China and obtained four value ranges of risk levels. This paper adopts green, yellow, orange, and red to represent the change in risk level from low to high based on the statistical results. Detailed values are shown in Table 1.

*3.3.2. Risk Coefficient Calculation Based on the Duration of Different Phases.* To describe the overall safety of the intersection, the risk coefficient $\delta$ is introduced as the comprehensive measurement, and its calculation formula is as follows:

$$\delta=\sum_{i=1}^{Z}\left(\alpha_{i1}\delta_{i1}+\alpha_{i2}\delta_{i2}\right),$$

$$\alpha_{ik}=\frac{T_{ik}}{C}, k=1,2, \tag{9}$$

Table 1: Risk level classification.

| Risk level | 1 | 2 | 3 | 4 |
|---|---|---|---|---|
| Conflict probability | 0~0.001 | 0.001~0.025 | 0.025~0.036 | ≥0.036 |
| Color | | | | |

where $\delta$ is the risk coefficient of the intersection, $\alpha_{i1}$ and $\alpha_{i2}$ are the proportion of the duration of phase switching stage and nonphase switching stage of phase $i$ in a signal period, respectively, and $\sum \alpha_{ik} = 1$. $\delta_{i1}$ and $\delta_{i2}$ are the risk coefficients of phase switching stage and nonphase switching stage in phase $i$, respectively, which can be obtained as follows:

$$\delta_{ik} = \sum_{j=1}^{4} \beta_j s_{ij}, k = 1, 2, \quad s_{ij} = \frac{n_{ij}}{m \times n}, \tag{10}$$

where $\beta_j$ is the weight of risk level $j$, which is used for risk calculation and analysis. The high-risk level is accompanied by large weight $\beta_j$. $s_{ij}$ represents the ratio of the number of cells with risk level $j$ to the total number of cells in phase $i$, and $n_{ij}$ represents the number of cells with risk level $j$ in phase $i$.

## 4. Model Verification

*4.1. Data Collection.* A SONY 4K HD camera was used to collect the traffic data of the intersection of Wushan Road and Yuehan Road in Guangzhou, China, from 16:00 to 18:00 on August 12, 2021. The collected parameters mainly include the geometric parameters of the intersection, the average speed of the traffic flow, traffic volume, steering ratio, large vehicle ratio, lateral deviation, time headway, and signal timing scheme. Among them, the geometric data of intersection is obtained by means of an artificial survey with a tape measure. The traffic speed is calculated by counting the time that the vehicles pass through the preset speed measuring interval after the green light (ignoring the first 5 vehicles), and the average value is taken. The calibration of all parameters is shown in Table 2. The signal timing scheme, traffic volume, steering ratio, large vehicle ratio, lateral deviation, and time headway are obtained through manual statistics. The signal timing scheme and traffic volume are shown in Table 3.

The data from the above table is input into the SICP model, and the heat maps of the predicted conflict probability distribution of four-phase stages are obtained, as shown in Figure 5. Figure 5(a) shows the heat map of traffic conflict probability in phase 1. At this time, part of the traffic flow on the north entrance of the previous phase does not completely leave the intersection, and the traffic flow on the east and west entrance is released at the same time. Figure 5(b) shows the heat map of traffic conflict probability in phase 2. The east-west traffic flow is normal, and the north traffic flow has completely left the intersection. Figures 5(c) and 5(d) show the heat map of traffic conflict probability in phase 3 and 4. Due to the setting of long full red time, the traffic flow at the east-west entrance has completely left the intersection, and only the traffic flow at the north entrance can pass normally.

*4.2. Comparison of Conflict Distribution Based on SSAM.* The VISSIM simulation model is established according to the geometric parameters, traffic flow parameters, and signal timing scheme of the intersection. Using the track file data output by VISSIM, traffic conflicts are analyzed in the surrogate safety assessment model (SSAM), as shown in Figure 6.

It can be found that the SICP model predicts the traffic conflict distribution of the intersection, and the result is consistent with SSAM. There are subtle differences between the two models, because the traffic conflicts of SSAM include rear-end conflicts, which are not within the scope of the SICP model. To verify the accuracy of the SICP model, sixteen conflict cells are selected on the heat maps of SICP and SSAM. The number of traffic conflicts is calculated by the SICP model and SSAM within an hour, as shown in Table 4. However, the conflict probability in this paper is defined as the probability that two or more vehicles arrive at the same cell during conflict time $t$. Thus, the number of traffic conflicts of a cell in an hour is that its conflict probability is multiplied by the number of conflict times.

From Table 4, it is found that the number of traffic conflicts between SSAM and SICP is similar in terms of the same conflict positions, and a little error is inevitable. The main reason for the difference is the lack of conflict sample size, and the prediction time is only one hour. If there are enough sample data, the SICP model will be better. However, the conflict number and the evolution trend of traffic conflicts given by the SICP model are close to those of SSAM, which indicates the effectiveness of the SICP model in terms of the prediction of traffic conflicts.

## 5. Case Study

To analyze the impact of typical optimization strategies on the safety level of intersections, this study adopts the SICP model to evaluate the risk status of intersections under three strategies, including nonsignalized strategies, signal timing optimization strategies, and traffic flow control strategies. A case study is conducted to provide feasible strategies for the safety optimization of nonsignalized or signalized intersections. This study takes the T-shaped intersection of Wushan road and Yuehan road in Guangzhou, China, as a case study. In this case, $\beta_j$ is set as 1, 3, 5, and 7 according to the risk level based on previous research experience [28, 31].

*5.1. Safety Analysis of Nonsignalized Strategy.* The SICP model is used to analyze the safety status of the case

Table 2: Parameter calibration.

| Parameter | Value | Explanation |
|---|---|---|
| $D$ $(m)$ | 3.75 | Lane width |
| $M$ $(m)$ | 21.5 | The length of intersection |
| $N$ $(m)$ | 22.5 | The width of intersection |
| $A$ $(m)$ | 0.5 | The width of the median |
| $B_1$ $(m)$ | 1.78 | The width of a small car |
| $L$ $(m)$ | 3.5 | The length of vehicle |
| $m$ | 40 | Cell rows |
| $n$ | 40 | Cell columns |
| $V_j$ (km/h) | 12.8 | Average speed |
| $S$ (pcu/h) | 1800 | Saturated flow rate |
| $\mu_1$ | 3.25 | Moment estimations of expectation of time headway |
| $\sigma_1^2$ | 10.32 | Moment estimations of variance of time headway |
| $\mu_2$ | 0.294 | The mean of the lateral deviation of straight or turning vehicles |
| $\sigma_2^2$ | 0.0098 | The variance of the lateral deviation of straight or turning vehicles |

Table 3: Traffic flow and signal timing parameters at the intersection of Wushan road and Yuehan road.

| Approach direction | East | | West | | North | |
|---|---|---|---|---|---|---|
| Symbol | E | | W | | N | |
| Lane function | Straight and right | Straight | Straight and left | Straight | Left | Right |
| Flow (pcu/h) | 358 | 484 | 324 | 416 | 43 | 108 |
| Large car ratio (%) | 20.16 | 7.02 | 5.99 | 27.44 | 0 | 0 |
| Turn ratio (%) | 8.7 | — | 18.66 | — | — | — |
| Phase | East-west | | | | North | |
| Green time(s) | 49 | | | | 22 | |
| Yellow time(s) | 3 | | | | 3 | |
| Full red time(s) | 25 | | | | 0 | |
| Cycle(s) | 102 | | | | | |

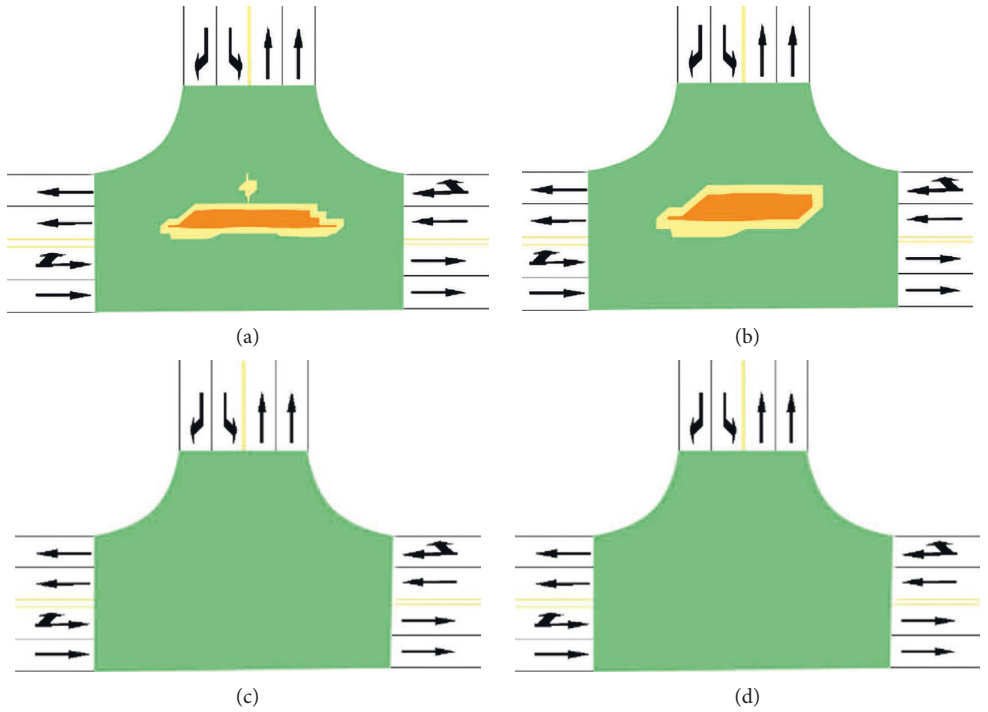


Figure 5: The heat map of the predicted conflict probability in different phases. (a) Phase stage 1. (b) Phase stage 2. (c) Phase stage 3. (d) Phase stage 4.

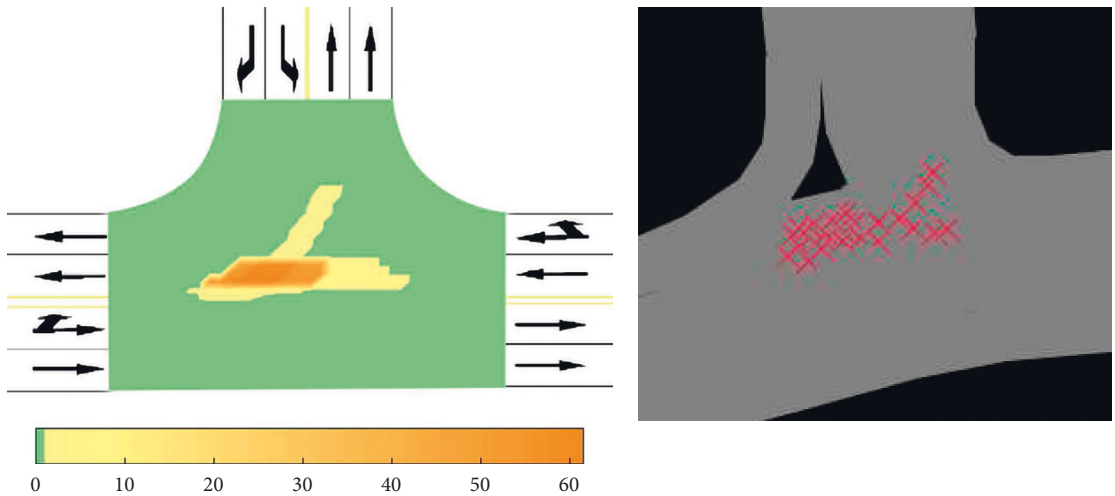


Figure 6: Comparisons between SSAM and SICP model. (a) The distribution of traffic conflict predicted by SICP. (b) The distribution of traffic conflict predicted by SSAM.

Table 4: Comparison of conflict number between SSAM and SICP model.

| Cell coordinate | SSAM | SICP |
|---|---|---|
| (−2, 2.5) | 60 | 59 |
| (−2.5, 2) | 69 | 62 |
| (−1.5, 1.5) | 74 | 62 |
| (3.5, −4.5) | 0 | 0 |
| (0, 5) | 4 | 2 |
| (5, 2) | 1 | 1 |
| (−3.5, 1.5) | 66 | 59 |
| (4.9, −2.5) | 0 | 0 |
| (−5, −2) | 0 | 0 |
| (−6, 1.5) | 51 | 52 |
| (−2,2) | 64 | 62 |
| (3, 5) | 2 | 1 |
| (5, 1.8) | 7 | 8 |
| (4.7, −3) | 0 | 0 |
| (3, 3) | 8 | 7 |
| (2, 1.5) | 6 | 8 |

intersection under the nonsignalized strategy and the existing signalized strategy and compare their difference in terms of the traffic conflict distribution. Due to the significant differences of vehicle arrival characteristics between the nonsignalized strategy and the signalized strategy, the Poisson distribution model is introduced to calculate the longitudinal arrival probability of vehicles in the SICP model [28, 31]. The heat maps of traffic conflict probability and conflict distribution under nonsignalized strategy at intersections are shown in Figure 7.

In Figure 7, the safety status of the signalized intersection changes with the signal phase, and the evolution of conflict probability and distribution area present with obvious periodicity, while the safety status of the nonsignalized intersection remains unchanged. In Figure 7(a), the traffic flow of each approach to the nonsignalized intersection can pass at any time. Thus, the traffic conflict probability of a nonsignalized intersection is static, and its conflict distribution is more intensive. Compared with phase 1 of the signalized strategy, the conflict distribution of intersection under the nonsignalized strategy is similar, but the value of the conflict probability is smaller. The conflict area of the intersection under the nonsignalized strategy is larger than that in phase 2 of the signalized strategy, but its conflict probability is smaller. The conflict area and conflict probability of intersection under the nonsignalized strategy are both larger than those in phases 3 and 4 of the signalized strategy. In Figure 7(b), the conflict distribution of nonsignalized intersection is partially different from that of the original signalized intersection, such that conflicts are more frequent and the severe conflict area is wider. In terms of the distribution and severity of traffic conflict, the safety level of an intersection under the signalized strategy is higher than that under the nonsignalized strategy.

*5.2. Safety Analysis of Signal Timing Optimization Strategy.* Based on the actual lane flow and the design conditions of the intersection, the mature Webster timing method is used to optimize the signal timing of the existing intersections. The signal timing parameters are shown in Table 5. The SICP model is taken to evaluate the safety status of the intersection after signal timing optimization. The heat map of conflict probability of intersection in different phases under the signal timing optimization strategy is given in Figure 8.

From Table 5, the signal timing scheme of the Webster method is quite different from the original signal timing scheme, which is mainly reflected in the all-red intervals and green split. The all-red intervals refer to the time when the traffic lights approaches of the intersection are red. The green split refers to the ratio of the green light time of each phase to the signal cycle. In terms of all-red intervals, there are two changes between two continuous phases. After the traffic flow in the east-west direction is released, the all-red intervals are shortened to improve traffic efficiency. Furthermore, all-red intervals of 3 seconds are newly added to clear the vehicles after the traffic flow in the north direction is released. In terms of phase time, the green split of each

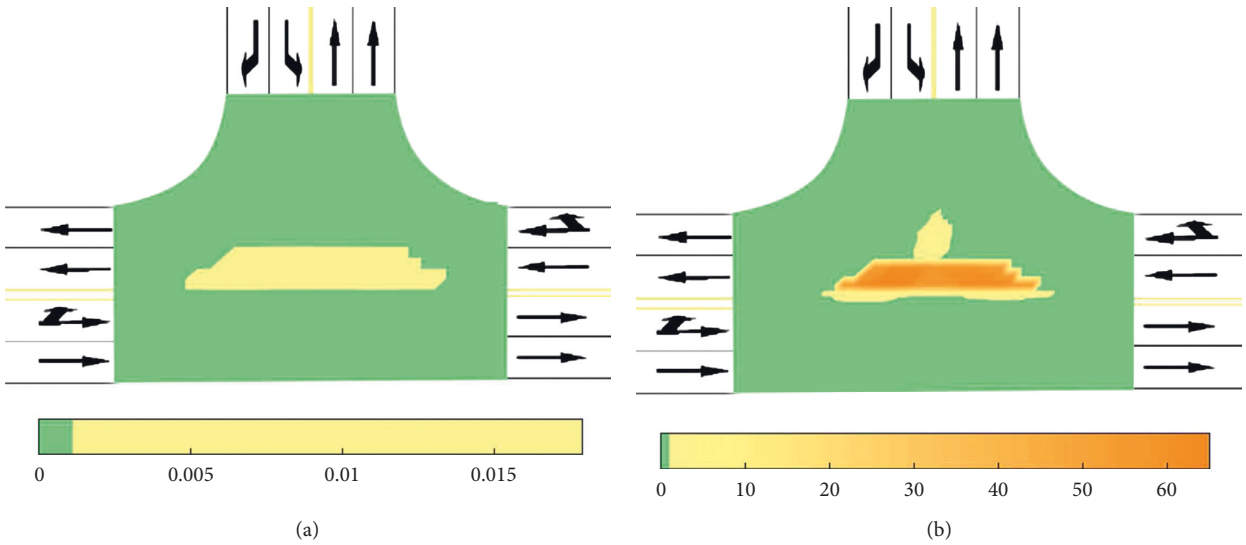


Figure 7: The traffic conflict probability and conflict distribution of intersection under nonsignalized strategy. (a) The heat map of traffic conflict probability. (b) Traffic conflict distribution in an hour.

Table 5: The signal timing parameters based on the Webster method.

| Approach direction | Lane function | Phase | Green time (s) | Yellow time (s) | Full red time (s) | Cycle (s) |
|---|---|---|---|---|---|---|
| East | Straight and right | East-west | 48 | 3 | 3 | 80 |
| | Straight | | | | | |
| West | Straight and left | | | | | |
| | Straight | | | | | |
| North | Left | North | 20 | 3 | 3 | |
| | Right | | | | | |

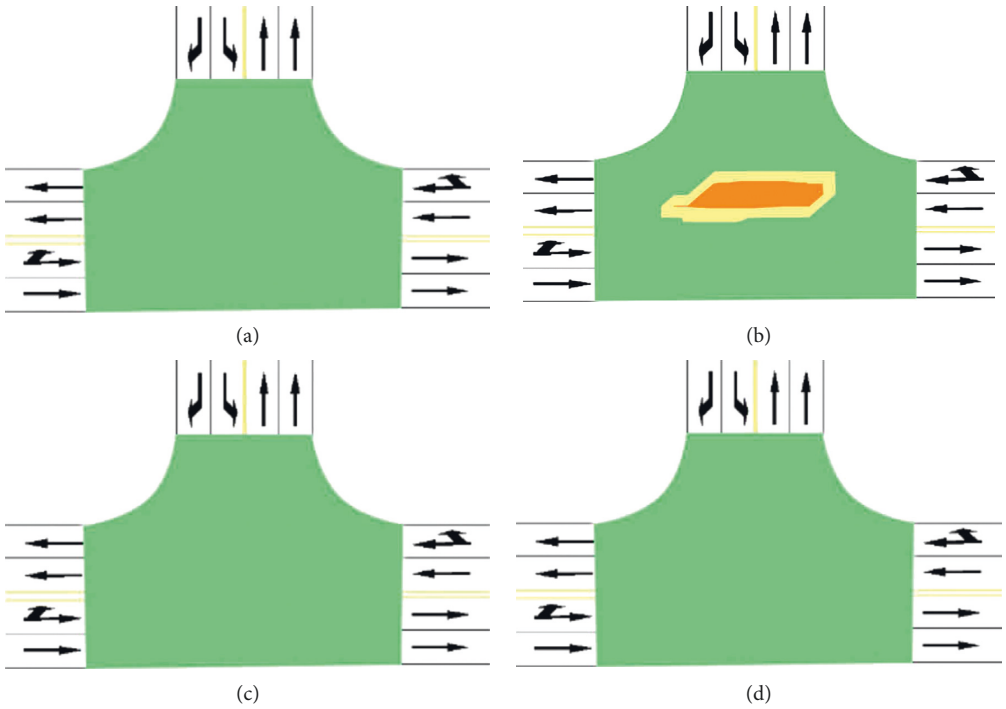


Figure 8: The heat map of conflict probability of intersection in different phases under signal timing optimization strategy. (a) Phase 1. (b) Phase 2. (c) Phase 3. (d) Phase 4.

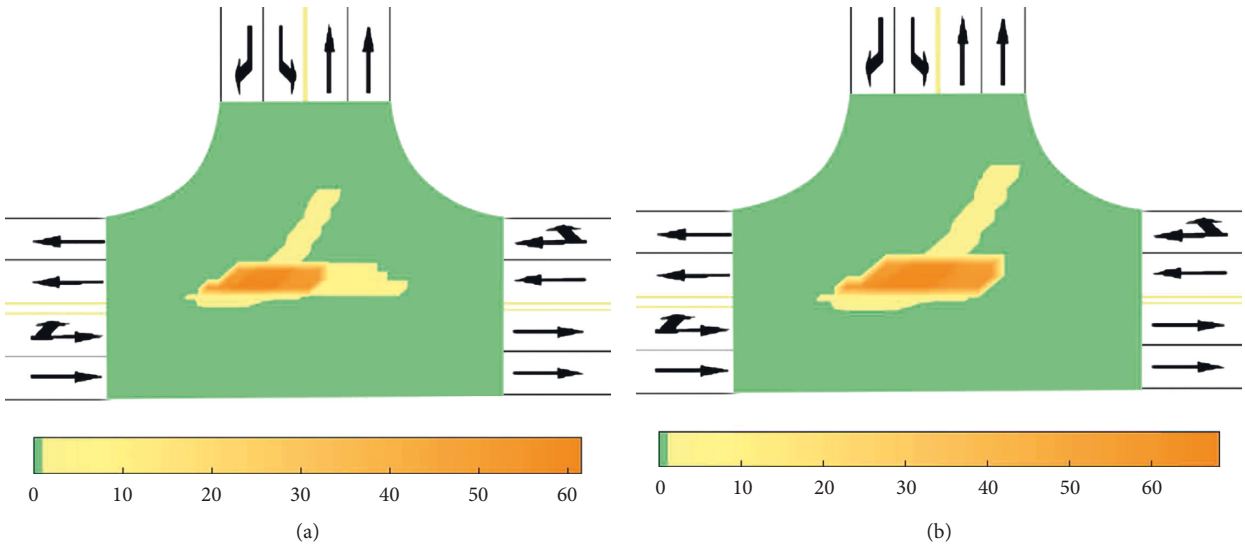


Figure 9: Conflict distribution of intersections before and after signal timing optimization. (a) Conflict distribution of intersection under original signal timing scheme. (b) Conflict distribution of intersection under the optimized signal timing scheme.

Table 6: Parameters and safety assessment of flow control measures (pcu/h).

| / | East approach | | West approach | | North approach | | / |
|---|---|---|---|---|---|---|---|
| Scheme | Straight and right | Straight | Straight and left | Straight | Left | Right | $\delta$ |
| 0 | 358 | 484 | 324 | 416 | 43 | 108 | 1.0465 |
| 1 | 251 | 339 | 324 | 416 | 43 | 108 | 1.0251 |
| 2 | 358 | 484 | 227 | 292 | 43 | 108 | 1.0451 |
| 3 | 358 | 484 | 324 | 416 | 31 | 76 | 1.0458 |

phase is positively correlated with the traffic flow. The larger traffic flow of the approach tends to go along with the larger green split of the associated phase.

From Figure 8, all red intervals of 3 seconds are added before phase 1, which avoids the traffic flow of the north approach leaving the intersection in time. The traffic conflicts between traffic flows of the north approach and the east-west approach in the original signal timing scheme are effectively eliminated. Thus, the conflict probability of phase 1 in the new signal timing scheme turns to zero. In other words, the conflict probability of the intersection is reduced after adopting the signal timing optimization scheme derived from the Webster method. The heat maps of the conflict distribution at intersections before and after signal timing optimization are shown in Figure 9.

In Figure 9, the conflict areas of the intersection under the optimized signal timing scheme significantly decline, and the conflict times slightly increase. The results show that the all-red intervals between two continuous phases can effectively cut down traffic conflict areas and improve the local safety of the intersection.

*5.3. Safety Analysis of Traffic Flow Control Strategy.* To analyze the internal mechanism between the traffic flow of the approach and the safety level of the signalized intersection, this paper adopts flow control measures for each approach. Flow control is a commonly used management and control measure in intersections and can be implemented by restricting and guiding the traffic flow at upstream intersections. Under the condition that the design speed of each approach remains unchanged, the traffic flow of different approaches is adjusted and outputs the associated heat map of conflict distribution. This case has designed 3 kinds of traffic flow control schemes, as shown in Table 6. Scheme 0 is the existing scenario. From scheme 1 to scheme 3, the traffic flow of the East, West, and North approaches is reduced by 30%.

The safety assessment results of each flow control scheme are obtained by implementing the SICP model, and the related heat maps of the conflict times are shown in Figure 10.

From Table 6 and Figure 10, the traffic flow control strategy helps to reduce the conflict area with risk levels 3 and 4. Compared with the existing scheme, the serious conflict areas in each scheme have been lessened to varying degrees. The greater the reduction in traffic flow, the better the optimization effect on the safety level of the entire intersection, such as scheme 1 and scheme 2. To further clarify the inherent relationship between the safety status of the intersection and the flow in each approach, the traffic flow of each approach increases from 0 to 3000pcu/h, and the numerical change in the risk coefficient at the intersection is shown in Figure 11.

From Figure 11, the risk coefficient of intersections presents a stepped growth trend with the increase in the

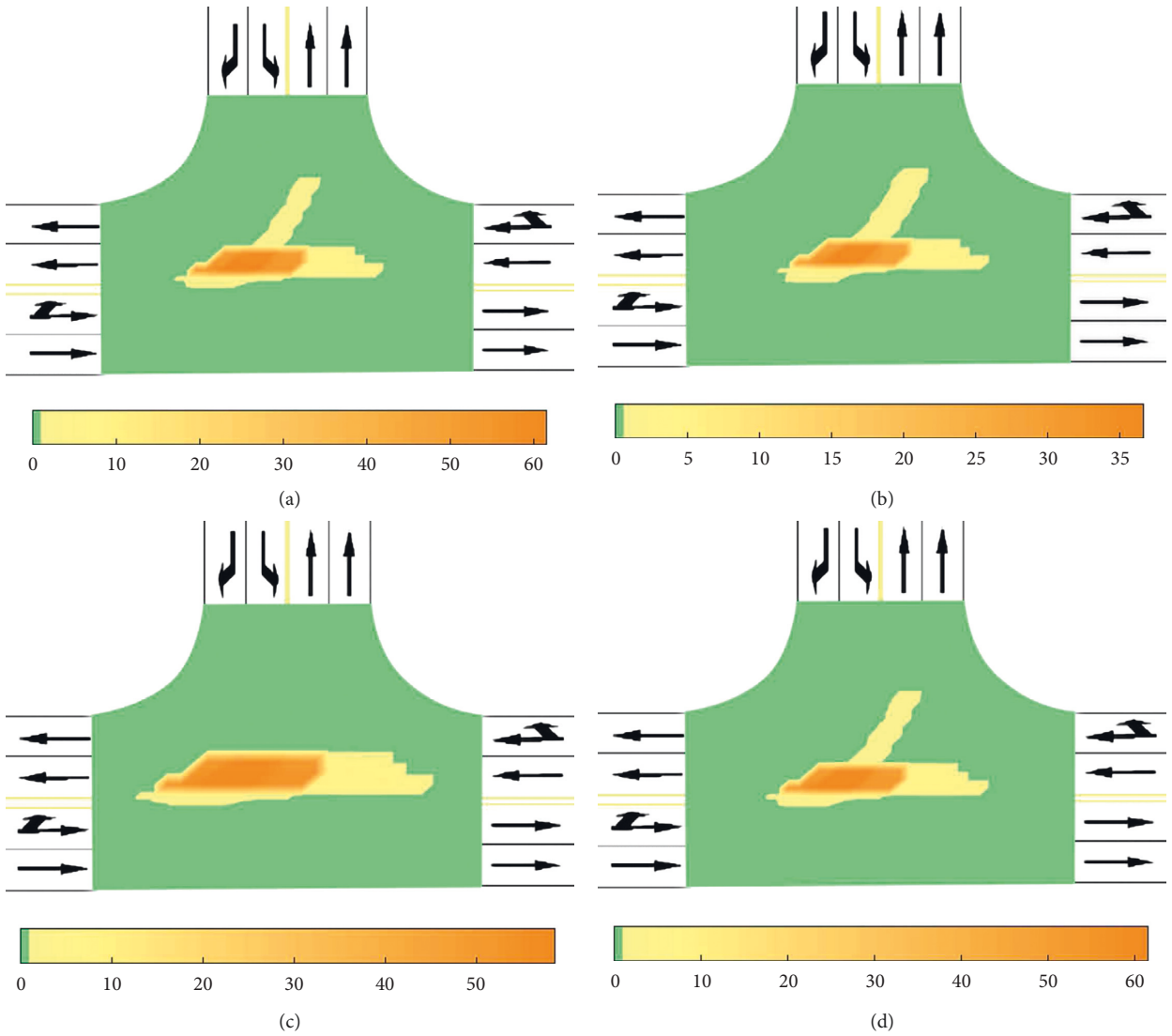


FIGURE 10: The heat maps of conflict times of intersection under different flow control schemes. (a) Existing scenario. (b) Scenario 1. (c) Scenario 2. (d) Scenario 3.

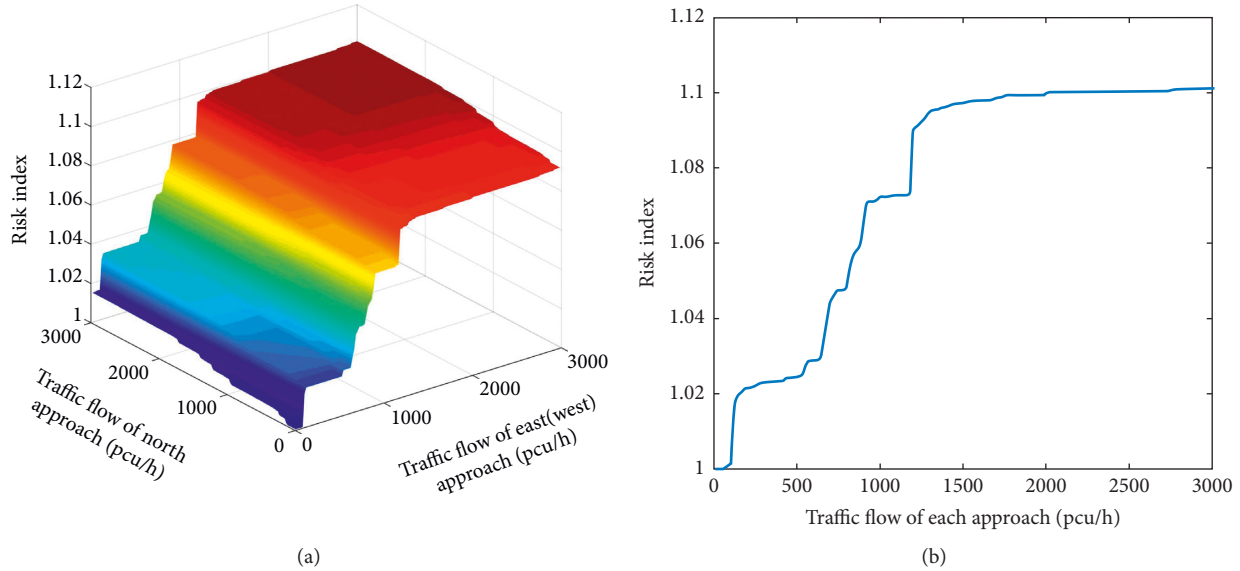


FIGURE 11: The relationship between risk index and traffic flow. (a) The relationship between risk index and the traffic flow of different approaches. (b) The relationship between risk factor and traffic flow of each approach.

traffic flow of each approach. In Figure 11(a), the risk coefficient is less affected by the changes in the traffic flow of the north approach and has a greater correlation with the traffic flow of the east-west approach. This means that the risk coefficient of the intersection is more influenced by the traffic flow of straight-left mixed lanes. In Figure 11(b), when the traffic flow of each approach increases from 0 pcu/h to 180 pcu/h, 520 pcu/h to 920 pcu/h, and 1180 pcu/h to 1300 pcu/h, the risk coefficient of the intersection rises rapidly. When the approach flow increased from 180 pcu/h to 52 0pcu/h, 920 pcu/h to 1180 pcu/h, and 1300 pcu/h to 3000 pcu/h, the growth rate of the risk coefficient tended to be flat. Therefore, when a signalized intersection is allowed to release straight and left-turn vehicles at the same time and the traffic flow in that approach is greater than 1300 pcu/h, the safety level of the intersection is less affected by an increase in traffic flow.

## 6. Conclusions

To address the problem of potential traffic conflict prediction at signalized intersections, this study proposes a safety assessment method that considers the impact of signal timing and does not rely on real-time and historical data. The micro motion characteristics of vehicles are introduced to construct a vehicle conflict probability prediction model. By collecting the traffic data of actual signalized intersections, the effectiveness of the model is verified. Furthermore, the safety state of intersections under the nonsignalized strategy, signal timing optimization, and flow control strategy is exploited to provide feasible safety improvement suggestions for traffic engineers. The research findings can be summarized as follows:

(i) The conflict probability of a signalized intersection tends to vary periodically with the change in phase, which cannot be described by the static safety assessment method.

(ii) Under the same conditions, the overall safety level of signalized intersections is higher than that of nonsignalized intersections, with fewer conflicts per unit time and smaller conflict areas.

(iii) The optimization of the signal timing scheme based on the Webster method is helpful to improve the safety of signalized intersections and effectively reduce the probability and number of traffic conflicts.

(iv) The risk coefficient of a signalized intersection is significantly affected by the traffic flow of straight and left mixed lanes and goes up with the increasing traffic flow. When the approach flow of the intersection is greater than a critical value, the growth rate of the risk coefficient tends to be stable.

Although some encouraging progress has been made, developing an appropriate safety assessment of signalized intersections with the high-precision prediction of traffic conflict is less successful and still requires further research. Due to the heterogeneity of intersection geometric conditions and drivers' driving habits, it is difficult to use a unified vehicle trajectory equation to summarize the vehicle trajectory at each approach. Thus, future research work will focus on improving the vehicle trajectory modeling of each approach. Additionally, the prediction effect of the SICP model is easily affected by parameter calibration and deserves further development. More traffic data of typical intersections will be introduced to calibrate the model in the future, to improve the prediction accuracy of the model.

## Data Availability

All data, models, or code that support the findings of this study are available from the corresponding author upon reasonable request.

## Conflicts of Interest

The authors declare that there are no conflicts of interest regarding the publication of this paper.

## Acknowledgments

The authors acknowledge Dianchen Zhu from the Hong Kong Polytechnic University for his valuable comments on this research. This paper was supported by the General Project of the National Natural Science Foundation of China (grant no. 52072129) and the Natural Science Foundation of Guangdong Province (grant no. 2018A030313250).

## References

[1] M. Ma, X. Yan, C. Wu, and H. Yin, "The effects of principal influential factors on traffic accident frequency at controlled intersections," *Journal of Jilin University (Engineering and Technology Edition)*, vol. 40, no. 2, pp. 417–422, 2010.

[2] M. He, X. Guo, Y. Chen, and L. Guo, "Application of improved gray clustering method in urban traffic safety assessment [J]," *Journal of Transport Information and Safety*, vol. 28, no. 1, pp. 104–107, 2010.

[3] A. C. Lorion and B. Persaud, "Investigation of surrogate measures for safety assessment of urban two-way stop controlled intersections," *Canadian Journal of Civil Engineering*, vol. 42, no. 12, pp. 987–992, 2015.

[4] A. S. Al-Ghamdi, "Analysis of traffic accidents at urban intersections in Riyadh," *Accident Analysis & Prevention*, vol. 35, no. 5, pp. 717–724, 2003.

[5] L. Guo, J. Zhou, S. Dong, and S. C. Zhang, "Analysis of urban road traffic accidents based on improved k-means algorithm," *China Journal of Highway and Transport*, vol. 31, no. 4, pp. 270–279, 2018.

[6] Y. Chen, H. Yuan, Z. Huang, and L. Wang, "Modeling intersection traffic crashes using a zero-truncated negative binomial model," *China Journal of Highway and Transport*, vol. 33, no. 4, pp. 146–154, 2020.

[7] U. Engel, "To what extent do conflict studies replace accident analysis: validation of conflict studies, an international review [C]. Organisme national," *de securite routiere Pmceedings of "Evaluation 85" Paris*, vol. 85, pp. 324–343, 1985.

[8] J. Glennon, "Critique of the traffic-conflict technique," *Transportation Research Record*, vol. 630, pp. 32–38, 1977.

[9] D. Migletz, W. Glauz, and K. Bauer, *Relationships between Traffic Conflicts and Accidents Volume I-Executive Summary*, Federal Highway Administration, USA, 1985.

[10] M. J. Williams, "Validity of the traffic conflicts technique," *Accident Analysis & Prevention*, vol. 13, no. 2, pp. 133–145, 1981.

[11] B. Zimolong and H. Erke, *Experimental Validation of Traffic Conflict Technique*, Technical University of Braunschweig, West Germany, 1977.

[12] C. Zegeer and R. Deen, "Traffic conflicts as a diagnostic tool in highway safety [J]. Transportation Research Record," *Journal of the Transportation Research Board*, vol. 667, no. 667, pp. 48–55, 1978.

[13] B. Zimolong, H. Erke, and H. Gstalter, *Traffic Conflicts at Urban Junctions: Reliability and Validity Studies*, University of Technology, Beijing, China, 1983.

[14] Y. Guo and M. T. M. M. S. Essa, "A comparison between simulated and field-measured conflicts for safety assessment of signalized intersections in Australia," *Transportation Research Part C: Emerging Technologies*, vol. 101, pp. 96–110, 2019.

[15] Y. Guo, T. Sayed, and M. Essa, "Real-time conflict-based Bayesian Tobit models for safety evaluation of signalized intersections," *Accident Analysis & Prevention*, vol. 144, Article ID 105660, 2020.

[16] Y. Guo, T. Sayed, and L. Zheng, "A hierarchical bayesian peak over threshold approach for conflict-based before-after safety evaluation of leading pedestrian intervals," *Accident Analysis & Prevention*, vol. 147, Article ID 105772, 2020.

[17] K. Gao, F. Han, P. Dong, N. Xiong, and R. Du, "Connected vehicle as a mobile sensor for real time queue length at signalized intersections," *Sensors*, vol. 19, no. 9, p. 2059, 2019.

[18] L. Hu, J. Ou, J. Huang, and F. Y. B. H. L. Wang, "Safety evaluation of pedestrian-vehicle interaction at signalized intersections in changsha, China," *Journal of Transportation Safety & Security*, pp. 1–26, 2021.

[19] L. Hu, X. Wu, J. Huang, and Y. W. Peng, "Investigation of clusters and injuries in pedestrian crashes using GIS in Changsha, China," *Safety Science*, vol. 127, Article ID 104710, 2020.

[20] V. Guttinger, "Conflict observation in theory and practice," in *Proceedings of the International Calibration Study of Traffic Conflict Techniques*, Berlin, Germany, 1984.

[21] C. Hyden and L. Linderholm, "The Swedish traffic-conflicts technique," in *Proceedings of the International Calibration Study of Traffic Conflict Techniques*, Springer Berlin, Heidelberg, Germany, January 1984.

[22] S. Kamijo and Y. K. M. Matsushita, "Traffic monitoring and accident detection at intersections," *IEEE Transactions on Intelligent Transportation Systems*, vol. 1, no. 2, pp. 108–118, 2000.

[23] T. Sayed and S. Zein, "Traffic conflict standards for intersections," *Transportation Planning and Technology*, vol. 22, no. 4, pp. 309–323, 1999.

[24] D. Gettman and L. Head, "Surrogate safety measures from traffic simulation models," *Transportation Research Record: Journal of the Transportation Research Board*, vol. 1840, no. 1, pp. 104–115, 2003.

[25] J. C. Hayward, "Near-miss determination through use of a scale of danger," *Highway Research Record*, vol. HRR384, 1972.

[26] B. Allen, B. Shin, and P. Cooper, "Analysis of traffic conflict and collisions [J]. Transportation Research Record," *Journal of the Transportation Research Board*, vol. 667, pp. 67–74, 1978.

[27] P. Cooper, "Experience with traffic conflicts in Canada with emphasis on "post encroachment time" techniques," in *Proceedings of the International calibration study of traffic conflict techniques*, Springer Berlin, Heidelberg, Germany, May 1984.

[28] Y. Ma, X. Qin, O. Grembek, and Z. Chen, "Developing a safety heatmap of uncontrolled intersections using both conflict probability and severity," *Accident Analysis & Prevention*, vol. 113, pp. 303–316, 2018.

[29] H. Park, C. Oh, J. Moon, and S. Kim, "Development of a lane change risk index using vehicle trajectory data," *Accident Analysis & Prevention*, vol. 110, pp. 1–8, 2018.

[30] C. Oh, S. Park, and S. G. Ritchie, "A method for identifying rear-end collision risks using inductive loop detectors," *Accident Analysis & Prevention*, vol. 38, no. 2, pp. 295–301, 2006.

[31] H. Wen, J. Wu, W. Qi, L. Wu, and K. Zhang, "CP-CS fusion model for on-ramp merging area in highway [J]," *Journal of South China University of Technology*, vol. 48, no. 2, pp. 50–57, 2020.

[32] E. Mohamed and S. Tarek, "Traffic conflict models to evaluate the safety of signalized intersections at the cycle level," *Transportation Research Part C*, vol. 89, pp. 289–302, 2018.

[33] yanyong Guo, *Signalized Intersection Safety Evaluation Techniques Based on Traffic Conflict Theory*, Southeast University, Bangladesh, 2016.

[34] Y. Ma, S. Qi, H. Wu, and L. Fan, "Traffic conflict identification model based on post encroachment time algorithm in ramp merging area," *Journal of Transportation Systems Engineering and Information Technology*, vol. 18, no. 2, pp. 142–148, 2018.

[35] A. Laureshyn, T. De Ceunynck, and C. Karlsson, "In search of the severity dimension of traffic events: extended Delta-V as a traffic conflict indicator," *Accident Analysis & Prevention*, vol. 98, pp. 46–56, 2017.

[36] C. Hyden, "The development of a method for traffic safety evaluation," *The Swedish Traffic Conflicts Technique*, Bulletin Lund Institute of Technology, Sweden, 1987.

[37] X. Jin, Y. Zhang, F. Wang, and L. D. Y. Z. Li, "Departure headways at signalized intersections: a log-normal distribution model approach," *Transportation Research Part C: Emerging Technologies*, vol. 17, no. 3, pp. 318–327, 2009.

[38] J. Wu, H. Wen, and W. Qi, "A new method of temporal and spatial risk estimation for lane change considering conventional recognition defects," *Accident Analysis & Prevention*, vol. 148, 2020.

[39] Y. Wang, S. Yang, and B. Pan, "Research of vehicle running track in highway straight section [J]," *Journal of Highway and Transportation Research and Development*, vol. 33, no. 2, pp. 111–119, 2016.

[40] Y. Pei, *Road Traffic Safety*, p. 253, China Communications Press, Beijing, China, 2007.